

Electronic structure and magnetism in $X_xW_{1-x}O_3$ ($X=Nb,V,Re$) from supercell calculations.

T. Jarlborg

Département de Physique de la Matière Condensée, Université de Genève, 24 Quai Ernest Ansermet, CH-1211 Genève 4, Switzerland

(June 12, 2018)

Some doped semiconductors have recently been shown to display superconductivity or weak ferromagnetism. Here we investigate the electronic structure and conditions for magnetism in a supercells of cubic $XW_{26}O_{81}$, where $X=Nb,V$ and Re . The undoped material is an insulator, and although the slightly doped material is a metal, it is far from the Stoner criterion of magnetism. The conditions of a localized density-of-states (DOS) which varies rapidly with the energy, resemble those of doped hexaborides. The virtual crystal approximation is used to vary the doping level. A small moment appears if the Fermi energy, E_F , coincides with a large derivative of the DOS.

I. INTRODUCTION.

Superconductivity and magnetism are expected to compete in materials having a large density-of-states (DOS) at E_F . However, recent studies of low DOS materials have found ferromagnetism (FM) of an unusual form, where a weak moment is combined with a surprisingly high Curie temperature, T_C . There are also examples of superconducting systems with a low DOS at E_F , since they are doped insulators¹⁻³. In particular, the quest of finding systems similar to the electron doped WO_3 , where small additions of Na are reported to make the system superconducting^{2,3}, suggests that hole doping should work as well. Instead, doping by dilute (2.5 %) Nb substitutions on W sites leads to weak itinerant ferromagnetism⁴, with properties not too different from those of doped hexaboride systems⁵. In this work we study the electronic structure of cubic $XW_{26}O_{81}$, with $X=Nb, V$ and Re , in order to see if similar conditions for magnetism are met as in La doped strontium hexaboride⁶.

The search for weak magnetism in metal doped oxide insulators is motivated by the hope that the correction of the Stoner factor by the Coulomb term⁶ should push some systems towards a FM state. The Stoner criterion for magnetism reads as follows when it is corrected for Coulomb energies;

$$\bar{S}_U = NI_s + U_0 N' N_v / N^2 \quad (1)$$

where I_s is the usual exchange integral^{7,8}, N is the density of states at E_F , N' is the energy derivative of the DOS of the impurity band, and N_v is the DOS of the remaining bands. The parameter U_0 is the Coulomb energy associated with a transfer of Δq electrons to the impurity. Magnetism is possible when $\bar{S}_U > 1$. It is only when the impurity band has a large energy derivative of the DOS, that charge transfers (CT) can be activated by an imposed exchange splitting. The last term of eq. 1 is negligible in most system, so that \bar{S}_U becomes the usual Stoner factor. But this term can be important because of various reasons. It depends on the sign of U_0 if the Stoner factor will increase or decrease because of the CT mechanism. It is difficult to calculate U_0 from a model DOS, because its value depends on self-consistent screening. But if the tendency follows eq. 1 one expects a large effect either because of large U_0 , N' and N_v , or because of low N^2 . If the background DOS is dominant we have $N_v \approx N$, so the condition is that $U_0 N' / N$ should be large. If an impurity band is formed at the band edge either below or above the gap in an insulator, one can expect a large ratio of N' / N because the total DOS will be small for small concentrations of impurities, while the slope of the DOS of the impurity band can be relatively high. The amplitude and sign of U_0 can depend on the dopant as well as on the host material. We will do self-consistent, spin-polarized calculations both for hole and electron doping. If the CT are opposite for the two types of doping and if U_0 is of the same sign for several types of dopants, one should find different behavior for the magnetic ordering.

II. METHOD OF CALCULATION.

The electronic structures are calculated using the self-consistent linear muffin-tin orbital method in the local spin density approximation^{9,10}. The calculations are made for the cubic, perovskite type structure of WO_3 , shown in figure 1. The oxygens occupy the face centered positions and the tungsten atom is at the center. No atoms occupy the open space at the cube corners, but the calculations include empty spheres at these positions. The supercell includes 27 elementary cells (or formula units, f.u.), where the 4-atom cells have been tripled along x, y and z. The exchange of one W with Nb is done in the central cell, making the concentration x close to 0.04. The calculations involve totally 135 sites

(108 atoms and 27 empty spheres) of which there are 14 nonequivalent ones. The basis-set includes s,p, and d for all sites, with f included in tails, and the bands are determined in 4 or 10 irreducible k-points. The virtual crystal approximation (VCA) is used in two cases with Nb as dopant. The nuclear charges and the number of electrons are increased to a non-integer number. As discussed later, each atom will receive 0.002 or 0.005 additional charges in VCA calculations with Nb as dopant. Other details of the calculations are the same as in the work on electron doping of WO_3 and SrTiO_3 ¹¹.

The real structure of $\text{Nb}_x\text{W}_{1-x}\text{O}_3$ in the experiment of Felner et. al.⁴ is tetragonal, where the concentration of Nb is lower ($x \approx 0.025$) than in the supercell here, and it may have some oxygen deficiency. The goal of the present work is not to study exactly the system used in the experiment, but to find out whether the conditions for weak ferromagnetism can be found in doped oxides as was found in some hexaborides⁶, and if such conditions can be expected to be frequent around impurities in metallic compounds. As will be shown, the result depend on details of the impurity DOS near E_F , so that magnetism appears to be correlated with a large derivative ("slope") of the DOS of the impurity band, as was found in the case of hexaborides. The conditions for this to happen in real materials are delicate. Large slopes of the DOS of the impurity band are needed and this can be a limiting case for very low impurity concentrations, when the size of the supercell and disorder of the real material will prohibitive for computations.

III. RESULTS.

The calculated DOS for $\text{NbW}_{26}\text{O}_{81}$ and undoped WO_3 ($\text{W}_{27}\text{O}_{81}$) near the valence band edge are shown in fig. 2. The band gap of about 2.1 eV for pure WO_3 is reduced to about 1.5 eV because of a separated NbO band complex just above the rest of the WO valence bands, and E_F enters into the valence band below the gap. A close up of the total DOS of $\text{NbW}_{26}\text{O}_{81}$ is shown in fig. 3, together with the partial DOS functions from the Nb impurity, from the six closest O, and from all W. The partial DOS functions show that the state just below the gap is very different from the uniform W-O mixture in the undoped system. The Nb impurity acts very differently from a W atom, and makes the p states on the nearest oxygens surrounding the impurity to become localized. It is seen from fig. 3 that about one third of the total DOS at E_F is coming from the six O-neighbors. The local DOS on the Nb impurity is only about 3 percent of the total DOS, cf. Table 1.

These results are very different from those of electron doping with Nb substitution on a Ti site in SrTiO_3 ¹¹. The local DOS on Nb and the surrounding oxygens in that case are very close to the respective DOS on Ti and O far away from the impurity. In other words, a rigid-

band model applies to Nb doping in SrTiO_3 , but not to Nb in WO_3 .

The moment tends to zero (or below $0.02 \mu_B/\text{cell}$) when one W is replaced with Nb. According to the mechanism of CT there should be a correlation between charge transfer, magnetic moment and the slope of the partial DOS at E_F . As seen in fig. 3, E_F is at a flat region of the DOS. In order to bring E_F into the negative slope of the DOS closer to the band edge, we use the VCA in two sets of calculations in order to add 0.002 and 0.005 electronic charges per atom. This adds 0.216 and 0.54 electrons per cell, respectively. This is a small amount of additional charge, and the paramagnetic DOS is almost identical to the one shown in fig. 3, except that E_F is moved a few mRy closer to the gap. The self-consistently calculated moment in the spin-polarized calculations tend to finite values in these cases. When 4 k-points are used we find about $0.72 \mu_B/\text{cell}$ when 0.216 electrons are added. This moment decreases when the calculations are continued using 10 k-points, but the moment becomes stable near $0.20 \mu_B/\text{cell}$, as seen in Table 1. These results confirm the mechanism of having a stabilizing effect from charge transfer when the band structure becomes spin polarized.

One calculation is made using 4 k-points in the case of 0.54 additional electrons, where E_F is moved closer to the gap. The value of N' is about twice as large at 0.54 as at 0.216 additional electrons, but the total DOS is lower, 88 instead of 102 states/Ry/cell. The spin-polarized calculation converges to a moment of about $0.28 \mu_B/\text{cell}$. This example seems to contradict the assumed correlation between N' and m (because the moment is lower than with 0.216 additional electrons), but it is clear that the relation does not hold for a vanishing DOS very close a gap, where nonlinear variations of the DOS becomes important.

Calculations for an impurity of V instead of a Nb give results in the DOS which are quite similar. But there are changes in details, which have an influence on the results for the magnetic moment. The smaller V atom makes the band edge different so that the DOS has a negative slope at E_F (cf. fig. 4 and Table 1) instead of being almost constant in the case of a Nb impurity. The DOS of the six oxygen atoms close to the V site is clearly negative and an increase of temperature or an imposed exchange splitting should decrease the charge on these atoms. Spin-polarized calculations give a considerable moment, about $0.92 \mu_B/\text{cell}$, when they are converged with 4 k-points. Note that this is without rigid-band shifts of E_F via VCA calculations. In the case of Nb it was not possible to find a stable moment unless a change in doping was forced by addition of 0.2 to 0.5 electrons per cell via the VCA.

Finally, a calculation is made for $\text{ReW}_{26}\text{O}_{81}$. It could be expected that the additional electron in Re (compared to W) will be added to the conduction band in a rigid band manner as for Nb in SrTiO_3 ¹¹. If so it could lead to an opposite condition for the correction to the Stoner factor, since N' should be positive. However, the results

from the band calculations show a very different situation. The Re-d band becomes localized just at the top of the valence band and hybridizes with O-p, as shown in fig. 5, instead of appearing at the bottom of the conduction band. The DOS near E_F is large on the impurity site (mainly Re-d). This is different to the cases of Nb and V as impurities, where the DOS on the impurity site is very small, while the six nearest oxygen sites take a significant part of the DOS. Other differences with the cases of Nb and V is that the derivatives of the total and partial DOS are varying rapidly with energy, and the amplitude of the total DOS is larger. From fig. 5 it is seen that N' near E_F is generally positive, even though a local peak just above E_F makes the conditions for charge transfer very complex. An increase of the temperature or an exchange splitting should mainly lead to a CT going in the opposite direction from what is the case with Nb or V impurity, although non-linearities are probable. This difference with Nb and V suggests that the magnetic state should not appear with Re as an impurity. Spin-polarized calculations using 4 k-points, where the self-consistent iterations start from an imposed large moment, converge towards a vanishing moment, smaller than $0.025 \mu_B/\text{cell}$. It can be concluded that no stable moment exists in this case.

IV. DISCUSSION.

These calculations show that there is a possibility of weak magnetic states around dopants of Nb and V in WO_3 , and as in the case of La dopant in hexaborides, there is a correlation between moment and sharp DOS structures of the impurity band. However, a notable difference with the hexaboride is that the impurities provoke a large localized DOS not on the impurity itself, but on the nearest oxygen sites, so that the O_6 band plays the role of impurity band. When there is a moment it is located (~ 80 percent of the total moment) to the O_6 cluster surrounding the impurity. These results suggest that the appearance of weak local moments can be quite common in many doped insulators. However, weak ferromagnetism are found at very low doping concentration in real, structurally distorted systems, and the present calculations are not exactly applicable for such systems. The present type of calculations demonstrate a mechanism behind the appearance of local moments, but whether the conditions of sharp DOS structures are sufficient for magnetism in each individual case is a delicate question. For instance, the previous study of La doped SrB_6 found a stable moment for a cell containing 8 formula units, while with one impurity in a 27 f.u. cell did not. A calculation with a rigid band shift of E_F within the VCA could restore favorable conditions for a small moment⁶. The Curie temperatures associated with the small moments are not yet understood within the present mechanism¹².

Semiconductors can be made magnetic by doping of

magnetic ions, like Mn in GaAs, where the magnetic RKKY interaction is believed to be responsible for the weak polarization of the host¹³. Band calculations using LDA for Mn impurities find a magnetic moment, which is localized on the Mn site¹⁴. This is somewhat different from the situation here, where a nonmagnetic ion make an insulating material weakly magnetic. The RKKY interaction might be essential for the polarization of the host, but the question is why the impurity or the closest neighbors become magnetic when the none of the ingredients (impurity and host) appear magnetic separately. This will be a Stoner-like case, where the DOS is such that the total energy is lower for the magnetic configuration, and this is irrelevant of having to deal with magnetic or nonmagnetic ions. It is through the DOS and the total energy of the compound that the magnetic state can be understood. A good example of this can be found in the calculated structural variation of magnetism in iron. The common bcc phase is magnetic, while in the fcc or hcp phases, at ambient or high pressure, the ground state is nonmagnetic. It is therefore not evident that Fe should be a magnetic in all host materials, like it is not evident that Nb as an impurity should cause magnetism in some cases.

In conclusion, from these results we propose that weak FM near impurities can be caused by a combination of exchange energy and charge transfer energy. The latter energy is favorable to spin splitting only under some precise conditions of the electronic structure near the impurity. This makes the appearance of such 'enhanced' Stoner magnetism rather circumstantial, and from the examples studied so far it can only produce small moments. The T-dependence of the moments is not expected to be anomalous and can not explain large Curie temperatures.

¹ Ch. J. Raub *et al.*, Phys. Rev. Lett. **13**, 1352 (1964).

² A. Aird and E.K.H. Salje, J. Phys.: Condens. Matter **10**, L377, (1998), A. Aird *et al.*, J. Phys.: Condens. Matter **10**, L569, (1998).

³ S. Reich and Y. Tsabba, Eur. Phys. J. B **9**, 1 (1999).

⁴ I. Felner, U. Asaf, M. Weger, S. Reich and G. Leituss, Physica B **311**, 191, (2002).

⁵ D.P. Young, D. Hall, M.E. Torelli, Z. Fisk, J.L. Sarrao, J.D. Thompson, H.R. Ott, S.B. Oseroff, R.C. Goodrich and R. Zysler, Nature **397**, 412 (1999).

⁶ T. Jarlborg, Phys. Rev. Lett. **85**, 186, (2000); T. Jarlborg, Physica B **307**, 291, (2001).

⁷ O. Gunnarsson, J. Phys. F **6**, 587 (1976); J.F. Janak, Phys. Rev. B **16**, 255, (1977).

⁸ T. Jarlborg and A. J. Freeman, Phys. Rev. B **22**, 2332, (1980).

⁹ O. K. Andersen, Phys. Rev. B **12**, 3060 (1975) ; T. Jarlborg

and G. Arbman, J. Phys. F **7**, 1635 (1977).

¹⁰ W. Kohn and L.J. Sham, Phys. Rev. **140**, A1133, (1965);
O. Gunnarsson and B.I Lundquist, Phys. Rev. B **13**, 4274,
(1976).

¹¹ T. Jarlborg, Phys. Rev. B **61**, 9887, (2000).

¹² T. Jarlborg, J. Phys.: Cond. Matter, **15**, L249, (2003).

¹³ M. Ohno, Science **281**, 951, (1998) and references therein.

¹⁴ J. König, J. Schliemann, T. Jungwirth and A.H. MacDonald,
cond-matt/0111314 (2001).

TABLE I. Dopant (X), valence charge (Q), total (N) and partial (on X) and O_6 , derivative of the total DOS (N'), and moments (m). The moments are calculated selfconsistently using 10 k-points for Nb and 4 for V and Re. There is no smooth variation of the DOS near E_F in the case of Re, and N' is not well defined. Results from VCA calculations are shown in the second line for one case with Nb doping, see the text.

X	Q	N	N_X	N_{O_6}	N'	m
	el./cell		(cell Ry) ⁻¹		(cell Ry ²) ⁻¹	μ_B /cell
Nb	647.0	106	3	36	-800	~ 0
Nb	647.2	102	3	35	-2900	0.20
V	647.0	145	3	88	-8200	0.98
Re	649.0	500	180	92	>0	~ 0

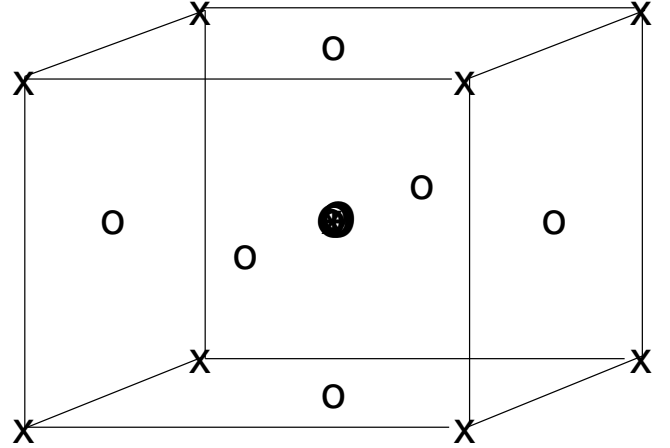


FIG. 1. The basic unitcell of cubic WO_3 . The oxygens are at the empty circles, the W at the filled circle, and empty spheres are included in the calculations at the positions of the crosses. The supercell in the calculations consists of 27 of the basic unit cells, with one of the W atoms replaced with an impurity site.

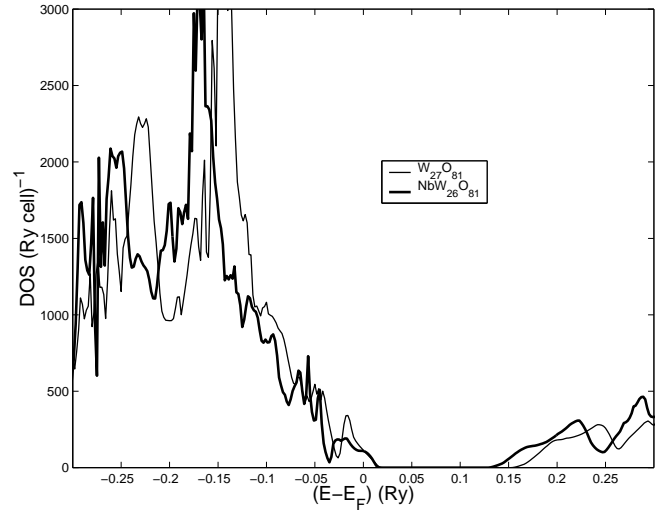


FIG. 2. Calculated DOS for $W_{27}O_{81}$ and $NbW_{26}O_{81}$ using 10 k-points in the irreducible Brillouin zone. The energies are aligned so that zero energy is at a band filling of 647 valence electrons in both cases. The Fermi energy is in the middle of the gap for the undoped and at zero energy for the doped case.

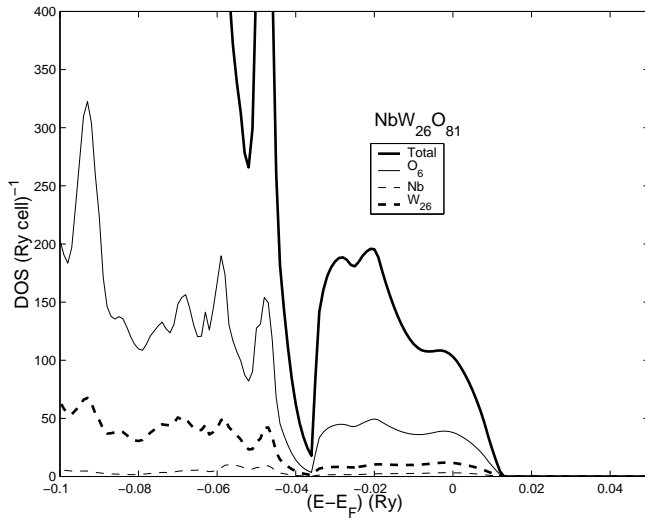


FIG. 3. Calculated DOS near E_F for $\text{NbW}_{26}\text{O}_{81}$ and the partial DOS from Nb, W_{26} and the six oxygen atoms closest to the Nb impurity. The DOS contains 1 electron between the position of E_F and the top of the valence band edge. Calculations in the virtual crystal approximation with 0.216 and 0.54 additional electrons put E_F more to the right, where the negative slope is large.

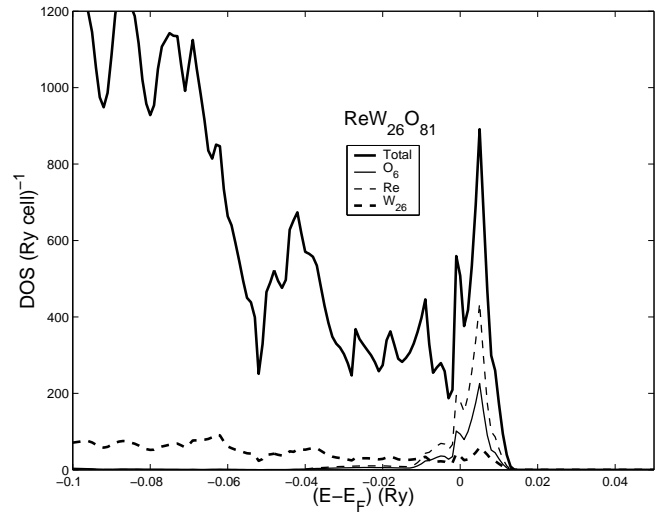


FIG. 5. Calculated DOS near E_F for $\text{ReW}_{26}\text{O}_{81}$ and the partial DOS from Re, W_{26} and the six oxygen atoms closest to the Re impurity. Note that the Re-d band forms an impurity band at the valence band edge, and thus the rigid band model does not apply in this case.

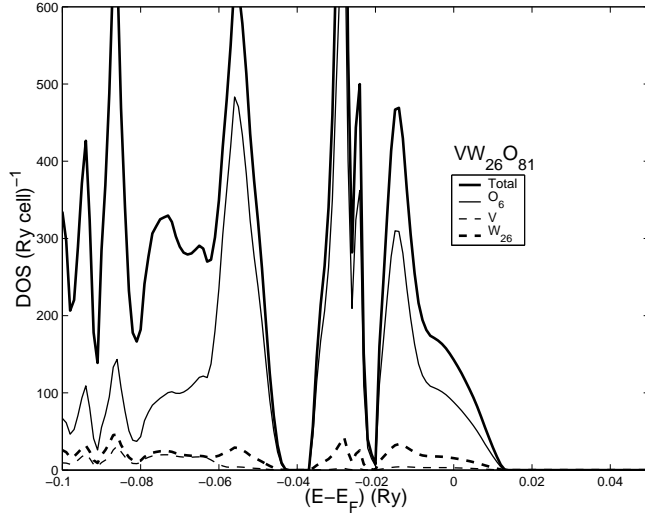


FIG. 4. Calculated DOS near E_F for $\text{VW}_{26}\text{O}_{81}$ and the partial DOS from V, W_{26} and the six oxygen atoms closest to the V impurity.